Precise quantum control of molecular rotation toward a desired orientation

Qian-Qian Hong [ORCID],[1] Daoyi Dong [ORCID],[2] Niels E. Henriksen [ORCID],[3] Franco Nori,[4,5] Jun He [ORCID],[1,*] and Chuan-Cun Shu [ORCID][1,†]

[1]*Hunan Key Laboratory of Nanophotonics and Devices, Hunan Key Laboratory of Super-Microstructure and Ultrafast Process, School of Physics, Central South University, Changsha 410083, China*
[2]*Australian Artificial Intelligence Institute, Faculty of Engineering and Information Technology, University of Technology Sydney, NSW 2007, Australia*
[3]*Department of Chemistry, Technical University of Denmark, Building 207, DK-2800 Kongens Lyngby, Denmark*
[4]*Quantum Computing Center and Theoretical Quantum Physics Laboratory, RIKEN, Saitama 351-0198, Japan*
[5]*Physics Department, University of Michigan, Ann Arbor, Michigan 48109, USA*

The lack of a direct map between control fields and desired control objectives poses a significant challenge in applying quantum control theory to quantum technologies. Here, we propose an analytical framework to precisely control a limited set of quantum states and construct desired coherent superpositions using a well-designed laser pulse sequence with optimal amplitudes, phases, and delays. This theoretical framework that corresponds to a multilevel pulse-area theorem establishes a straightforward mapping between the control parameters of the pulse sequence and the amplitudes and phases of rotational states within a specific subspace. As an example, we utilize this approach to generate 15 distinct and desired rotational superpositions of ultracold polar molecules, leading to 15 desired field-free molecular orientations. By optimizing the superposition of the lowest 16 rotational states, we demonstrate that this approach can achieve a maximum orientation value of $|\langle\cos\theta\rangle|_{\max}$ above 0.99, which is very close to the global optimal value of 1 that could be achieved in an infinite-dimensional state space. This work marks a significant advancement in achieving precise control over multilevel subsystems within molecules. It holds potential applications in molecular alignment and orientation, as well as in various interdisciplinary fields related to the precise quantum control of ultracold polar molecules, opening up considerable opportunities in molecular-based quantum techniques.

Introduction. Owing to the inclusion of vibrational and rotational degrees of freedom, molecular systems offer exceptional opportunities for encoding quantum information beyond the capabilities of other platforms [1–4]. Advancements in experimental techniques, theoretical models, and computational methods have led to significant progress in quantum control of molecular rotation in recent years [5–10]. One of the main goals in this field is to develop advanced methods for achieving molecular orientation without the need for external static fields [11–17]. The physical mechanism for this phenomenon involves generating rotational wave packets consisting of both even and odd angular momentum quantum numbers. This capacity holds immense potential across a diverse range of applications, including photochemistry [18,19], precision spectroscopy [20,21], ultrafast science [22–25], molecular imaging [26–28], quantum information processing [29], and material science [30,31].

Quantum control techniques, particularly with the use of shaped laser pulses, have made it possible to harness the rotational states of molecules as the fundamental units, referred to as qubits, for performing quantum computing and simulations [32–37]. This approach allows for the encoding, manipulating, and measuring of qubits within a finite-dimensional space of rotational states [38–41]. In light of this progress, an intriguing question arises: Is it feasible to exert precise control over a specific subset of rotational states to achieve a desired field-free orientation of molecules? It requires accurately determining the amplitude and phase of the wave function for each involved rotational state. Despite significant progress in experimental techniques and theoretical methods for controlling quantum systems [42–46], establishing a straightforward analytical approach to uncover the intricate relationship between control fields and rotational wave functions remains a complex task in quantum control. This complexity can be attributed to the involvement of multiple rotational states and complex transitions.

In this Letter, our primary goal is to establish an analytical framework that can effectively address the complexities of achieving precise control over a given number of rotational states and ultimately achieve any desired rotational superposition. Through the analytical design of a pulse sequence, we derive a general multilevel pulse-area theorem that accurately maps characteristic parameters of each

---

*Contact author: junhe@csu.edu.cn
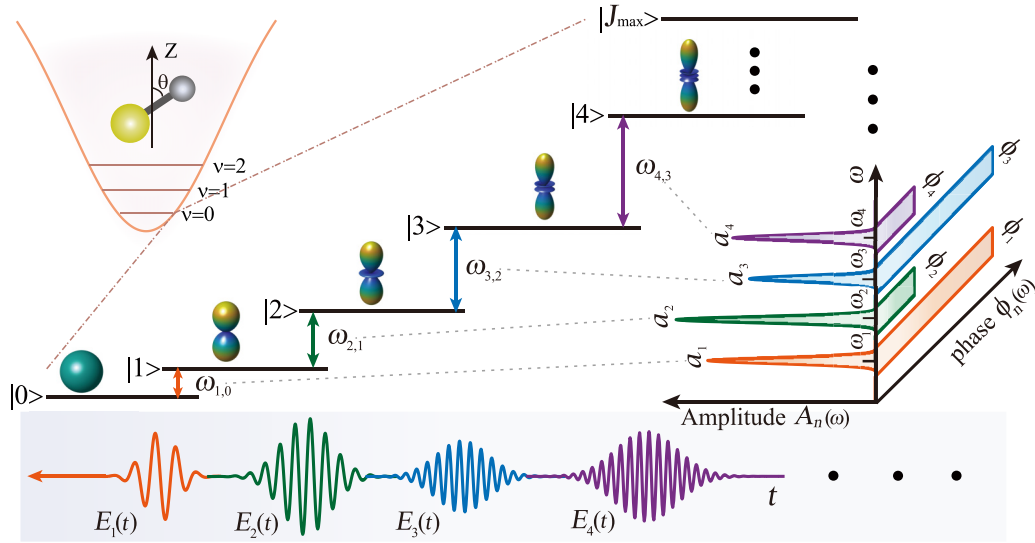†Contact author: cc.shu@csu.edu.cn

FIG. 1. Schematic illustration of generating a desired coherent superposition of rotational states of ultracold polar molecules initially in the absolute ground state ($v = 0$ and $J = 0$) of the ground electronic potential by a precisely designed pulse sequence. The subspace consists of a finite number of rotational states, which is driven from the ground state $|0\rangle$ to the highest rotational state $|J_{max}\rangle$ step by step by a time-domain optimized pulse sequence, analytically designed in the frequency domain by control parameters $\{a_n, \phi_n, \omega_n\}$.

subpulse, such as amplitude, phase, time delay, and center frequency, onto the excited rotational wave packet of molecules. To validate our theoretical method, we perform numerical simulations to confirm that the analytically designed pulse sequence can achieve precise control over a finite number of rotational states of ultracold dipolar molecules in their absolute ground state and work toward attaining a desired field-free molecular orientation. This theoretical framework holds promising implications for molecular-based quantum techniques.

Precise control method. We now explain how to establish a general precise control method based on pulse sequence excitation. Figure 1 illustrates our control scheme for manipulating rotational quantum states of ultracold dipolar molecules using a linearly polarized pulse sequence

$$E(t) \equiv \sum_{n=1}^{N} E_n(t) = \sum_{n=1}^{N} \mathcal{E}_n f_n(t) \cos[\omega_n(t - \tau_n) + \phi_n], \quad (1)$$

where $\mathcal{E}_n$ denotes the electric field's amplitude, $f_n(t)$ the envelope function, ω_n the center frequency, τ_n the center time, ϕ_n the phase of the nth subpulse $E_n(t)$, and N the total number of subpulses. By carefully designing each subpulse with specific parameters, the objective of this approach is to transfer the molecules from the ground rotational state $|J = 0\rangle$ in the ground vibrational state of the ground electronic state at the initial time t_0 to a target subspace of rotational states at the final time t_f defined by ($\hbar = 1$)

$$|\psi(t_f)\rangle = \sum_{J=0}^{J_{max}} c_J \exp(i\varphi_J) \exp(-i\omega_J t_f)|J\rangle, \quad (2)$$

where ω_J represents the eigenfrequency, c_J the real positive amplitude, φ_J the phase of the rotational state $|J\rangle$ with rotational quantum number J, and J_{max} the highest rotational state in the subspace.

To establish a mapping between the control parameters $\{\mathcal{E}_n, \omega_n, \tau_n, \phi_n\}$ and the quantum state parameters $\{c_J, \varphi_J\}$, we elucidate our approach by investigating the impact of a single pulse on a two-level system, commonly known as a single qubit. This analysis led to the identification of Rabi oscillations and the concept of the π-pulse [47–50]. Here, the two-level system is composed of $|0\rangle$ and $|1\rangle$ with a transition dipole moment $\mu_{1,0}$ and a transition frequency $\omega_{1,0} = \omega_1 - \omega_0$. By employing the first-order Magnus expansion of the unitary time-evolution operator, the time-dependent wave function of the system in the interaction picture reads [51]

$$|\psi(t)\rangle_1 = \cos \theta_1(t)|0\rangle + i \sin \theta_1(t) \exp[-i(\phi_1 - \omega_1 \tau_1)]|1\rangle, \quad (3)$$

where the pulse area $\theta_1(t)$ is given by $\theta_1(t) = \mu_{1,0}|\int_{t_0}^{t} E_1(t') \exp(-i\omega_{1,0}t')dt'|$. By employing the frequency-domain analysis of the control pulse $E_n(t) = \frac{1}{\pi} \text{Re}[\int_0^\infty A_n(\omega) \exp[i(\phi_n - \omega\tau_n)] \exp(i\omega t)d\omega]$, where $A_n(\omega)$ denotes the spectral amplitude and $\phi_n(\omega)$ represents the spectral phase, we can deduce that the pulse area $\theta_1(t_f)$ is solely determined by $A_1(\omega)$ at $\omega_{1,0}$. By considering resonant excitation with $\omega_1 = \omega_{1,0}$, we can ensure that the value of $\theta_1(t_f)$ is precisely controlled by the control parameter $\mathcal{E}_1$. As a result, this has given rise to a well-established two-level pulse-area theorem, which allows for precise manipulation of the control parameters $\mathcal{E}_1$ and ϕ_1. This manipulation can be used to generate an arbitrary coherent superposition of two states, serving as the fundamental unit of quantum information and holding considerable significance in quantum techniques.

While various quantum optimal control theory methods have been successfully applied to finding optimal external fields [52–56], deriving the analytical solution for the time-dependent wave function of a multilevel system is generally more complex than that of a two-level system [57,58]. This complexity necessitates the advancement of a multilevel

pulse-area theorem for precise control of high-dimensional quantum systems. We have made strides toward this ultimate goal by examining various three-level models [59–61]. Through the utilization of pure rotational ladder-climbing excitations between states, we established the mapping of control amplitudes $\mathcal{E}_1$ and $\mathcal{E}_2$, as well as control phases ϕ_1 and ϕ_2, onto the amplitudes and phases of three rotational states [60]. Here, we analyze a pulse sequence that comprises a series of subpulses distributed at specific time intervals. By considering each subpulse that couples two adjacent rotational states independently, as depicted in Fig. 1, we derive a general solution of the time-dependent wave function comprising multiple rotational states without invoking the rotating wave approximation (RWA) [62]

$$
\begin{aligned}
|\psi(t)\rangle_N = {} & \cos\theta_1(t)|0\rangle + \sum_{J=1}^{N-1}\cos\theta_{J+1}(t)\prod_{n=1}^{J} i\sin\theta_n(t) \\
& \times \exp[-i(\phi_n - \omega_{n,n-1}\tau_n)]|J\rangle \\
& + \prod_{n=1}^{N} i\sin\theta_n(t)\exp\left[-i(\phi_n - \omega_{n,n-1}\tau_n)\right]|J_{\max}\rangle,
\end{aligned}
$$
(4)

where the subpulse area is defined as $\theta_n(t) = \mu_{n,n-1}|\int_{t_0}^{t} E_n(t')\exp(-i\omega_{n,n-1}t')dt'|$, with the dipole transition matrix element $\mu_{n,n-1}$ and the transition frequency $\omega_{n,n-1} = \omega_n - \omega_{n-1}$ from the nth rotational state to the $(n-1)$th rotational state. The values of the transition dipole matrix element between $|J+1\rangle$ and $|J\rangle$ are given by $\mu_{J+1,J} = \mu_0 \mathcal{M}_{J+1,J}$, with the permanent dipole moment μ_0 and the transition matrix element $\mathcal{M}_{J+1,J} = (J+1)/\sqrt{(2J+3)(2J+1)}$.

Based on Eq. (4), we can analyze how the control parameters are mapped onto the wave function of rotational states. As an example, we consider the nth subpulse that has a Gaussian frequency distribution given by $A_n(\omega) = a_n\exp[-(\omega - \omega_n)^2/2\Delta\omega_n^2]$, where a_n represents the amplitude, ω_n the center frequency, and $\Delta\omega_n$ the bandwidth. The time-dependent pulse sequence $E(t)$, capable of generating the coherent superposition of rotational states as described in Eq. (4), can be obtained by

$$
E(t) = \sum_{n=1}^{N}\sqrt{\frac{2}{\pi}}\frac{1}{T_n}\frac{\theta_n(t_f)}{\mu_{n,n-1}}e^{-\frac{(t-\tau_n)^2}{2T_n^2}}\cos[\omega_{n,n-1}(t-\tau_n)+\phi_n],
$$
(5)

with the subpulse duration $T_n = 1/\Delta\omega_n$ and the electric field's amplitude $\mathcal{E}_n = \sqrt{2/\pi}\theta_n(t_f)/(T_n\mu_{n,n-1})$ compared with its definition in Eq. (1). Through precise modulation of the control parameters, it becomes possible to manipulate an arbitrary high-dimensional superposition of rotational states described by Eq. (4) to a desired target state defined in Eq. (2). This approach can potentially manipulate rotational states, creating a larger state space to store and process information for high-dimensional quantum simulation.

Application to the generation of desired molecular orientation. As an example, we now analytically design a pulse sequence described by Eq. (5) to maximize the degree of orientation within a subspace of rotational states with optimal state parameters $\{c_n, \varphi_n\}$ by optimizing control parameters

$\{\mathcal{E}_n, \phi_n, \tau_n\}$. By considering the rotational excitations, the degree of orientation at the final time t_f can be quantified by

$$
\langle\cos\theta\rangle(t_f) = 2\sum_{J=0}^{J_{\max}-1} c_{J+1}c_J \mathcal{M}_{J+1,J}\cos(\omega_{J+1,J}t_f - \varphi_{J+1,J}),
$$
(6)

where θ represents the angle between the field polarization direction and the molecular axis, as depicted in Fig. 1, and $\varphi_{J+1,J} = \varphi_{J+1} - \varphi_J$ represents the relative phase difference between $|J+1\rangle$ and $|J\rangle$. The values of $\langle\cos\theta\rangle(t_f) = \pm 1$ indicate perfect orientation and perfect antiorientation, respectively, while an isotropic distribution signifies $\langle\cos\theta\rangle(t_f) = 0$.

Due to the complexities involved in matrix diagonalization, deriving the analytical eigenvalues and eigenvectors of the operator $\cos\theta$ becomes increasingly challenging for systems that are more complex than simple two- and three-level systems. By utilizing the method of Lagrange multipliers [63,64], the maximum degree of orientation, i.e., $\lambda \equiv |\langle\cos\theta\rangle|_{\max}$, at full revivals for a given value of $J_{\max}$ can be determined by solving the following equation [62]:

$$
\begin{aligned}
& \lambda^{J_{\max}+1} \\
& + \sum_{k=1}^{[\frac{J_{\max}+1}{2}]}(-1)^k\left\{\prod_{n=1}^{k}\sum_{l_1=0;l_n=l_{n-1}+2}^{J_{\max}-1-2k+2n}\mathcal{M}_{l_n+1,l_n}^2\right\}\lambda^{J_{\max}+1-2k} = 0,
\end{aligned}
$$
(7)

where $[\frac{J_{\max}+1}{2}]$ represents the greatest integer less than $\frac{J_{\max}+1}{2}$. The state amplitudes and phases in the target subspace by Eq. (2) should satisfy the following relations:

$$
\begin{aligned}
c_J = {} & \frac{\lambda^J + \sum_{k=1}^{[J/2]}(-1)^k\left\{\prod_{n=1}^{k}\sum_{l_1=0;l_n=l_{n-1}+2}^{J-2k+2(n-1)}\mathcal{M}_{l_n+1,l_n}^2\right\}\lambda^{J-2k}}{\prod_{l=0}^{J-1}\mathcal{M}_{l+1,l}} \\
& \times c_0
\end{aligned}
$$
(8)

and

$$
\varphi_{J+1} - \varphi_J = (J+1)(\varphi_1 - \varphi_0) + 2k\pi, \quad (k = 0, \pm 1, \pm 2\cdots),
$$
(9)

with the constraint $\sum_{J=0}^{J_{\max}} c_J^2 = 1$.

By combining the optimal amplitudes and phase conditions with the analytical wave function in Eq. (4), we can design the pulse sequence in Eq. (5) with optimal control parameters

$$
\theta_1(t_f) = \arccos c_0,
$$
$$
\theta_n(t_f) = \arccos\frac{c_{n-1}}{\left|\prod_{k=1}^{n-1} i\sin\theta_k(t_f)\exp\left[-i(\phi_k - \omega_{k,k-1}\tau_k)\right]\right|},
$$
$$
(1 < n \leqslant N)
$$
(10)

and

$$
\phi_n = \omega_{n,n-1}\tau_n - n(-\phi_1 + \omega_{1,0}\tau_1) - \frac{(n-1)\pi}{2} + 2k\pi,
$$
$$
(n > 1),
$$
(11)

for any initial phase ϕ_1. We can use the optimal pulse area $\theta_n(t_f)$ to calculate the control parameter $\mathcal{E}_n$ of the nth subpulse in Eq. (1). This approach explicitly establishes a mathematical
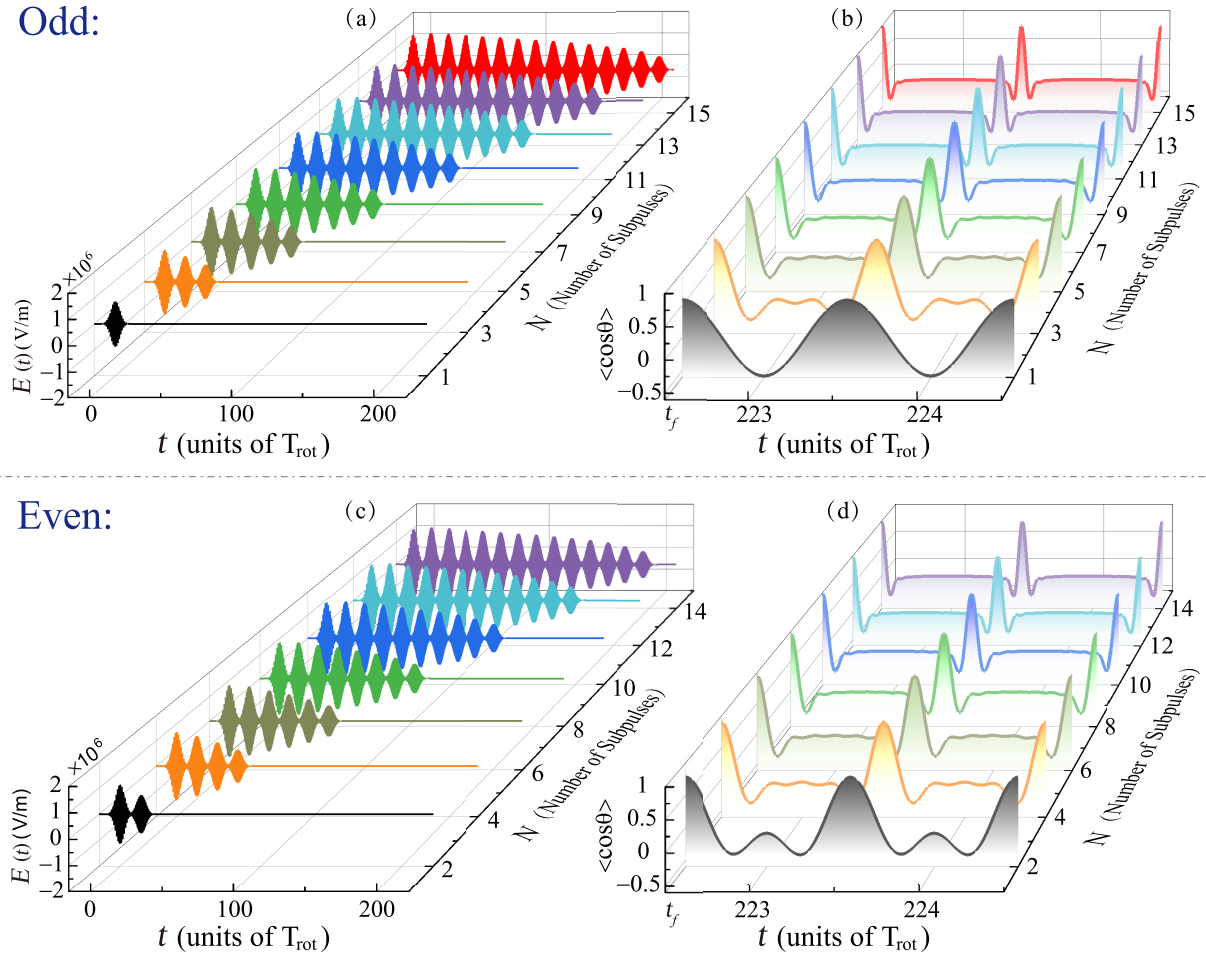
FIG. 2. The analytically designed pulse sequence (a and c) and the corresponding degree of orientation $\langle \cos \theta \rangle$ (b and d) within different subspaces with odd and even numbers of subpulses $N = J_{\max}$. The time is measured in units of the full revival period $T_{\text{rot}} = \pi/B = 2.2$ ps of the LiH molecule. All pulse sequences used in our simulations are turned on at the initial time $t_0 = -15T_{\text{rot}}$ and off at the final time $t_f = 222.5T_{\text{rot}}$ marked in (b) and (d).

mapping that allows for constructing a desired superposition of multirotational states in the target subspace by controlling three parameters $\{\mathcal{E}_n, \phi_n, \tau_n\}$, which can maximize the degree of orientation at full revivals for a given value of $J_{\max}$.

Numerical simulations for ultracold polar molecules. We conduct numerical simulations for ultracold polar molecules initially in the rovibrational ground state of the ground electronic state, which can be obtained under the current experimental conditions [65–67]. As an example, we consider ultracold LiH molecules with a rotational constant $B = 7.513$ cm^{-1} and a permanent dipole moment $\mu_0 = 5.88$ D. Since our method requires each subpulse with a sufficiently long duration T_n for satisfying the resonance conditions, we fix the duration of all subpulses at $T_n = 3T_{\text{rot}}$ with $T_{\text{rot}} = \pi/B = 2.2$ ps [62]. By fixing the center time of $\tau_n = 5(n-1)T_n$, we use Eqs. (10) and (11) to determine the control parameters $\{\mathcal{E}_n, \phi_n\}$ for a given value of $N = J_{\max}$, which are then substituted into Eq. (5) to obtain the analytically designed pulse sequence $E(t)$. To calculate the time-dependent rotational wave function $|\psi(\theta, t)\rangle$, we numerically solve the corresponding time-dependent Schrödinger equation governed by the Hamiltonian $\hat{H}(t) = B\hat{J}^2 - \mu_0 E(t) \cos \theta$ [68]. The degree of orientation $\langle \cos \theta \rangle(t)$ is then calculated by

$\langle \cos \theta \rangle(t) = \langle \psi(\theta, t) | \cos \theta | \psi(\theta, t) \rangle$, without making use of the approximations employed in our analytical derivations.

Figure 2 shows the time-dependent degree of orientation $\langle \cos \theta \rangle(t)$ induced by the analytically designed pulse sequence, as described in Eq. (5), with N ranging from 1 to 15 in odd numbers for Figs. 2(a) and 2(b) and even numbers for Figs. 2(c) and 2(d) to avoid the clutter of multiple lines. As depicted in the plot, the analytically designed pulse sequence with a given number of subpulses N in Figs. 2(a) and 2(c) can achieve the desired maximum degree of orientation, aligning with the theoretical values derived from Eq. (7). The maximum degree of orientation for one pulse is 0.5774 by including the lowest two rotational states, which has been experimentally demonstrated [69] by using a long nonresonant laser pulse and a weak static electric field. By increasing the number of subpulses in the pulse sequence and modulating their amplitudes and phases, the maximum degree of orientation gradually increases. When we use such a pulse sequence that consists of 15 subpulses to optimize the superposition of the lowest 16 rotational states, the maximum degree of orientation can reach 0.99, approaching perfect orientation. The time-dependent orientation behavior induced by the designed pulses exhibits quantum revivals at regular intervals of
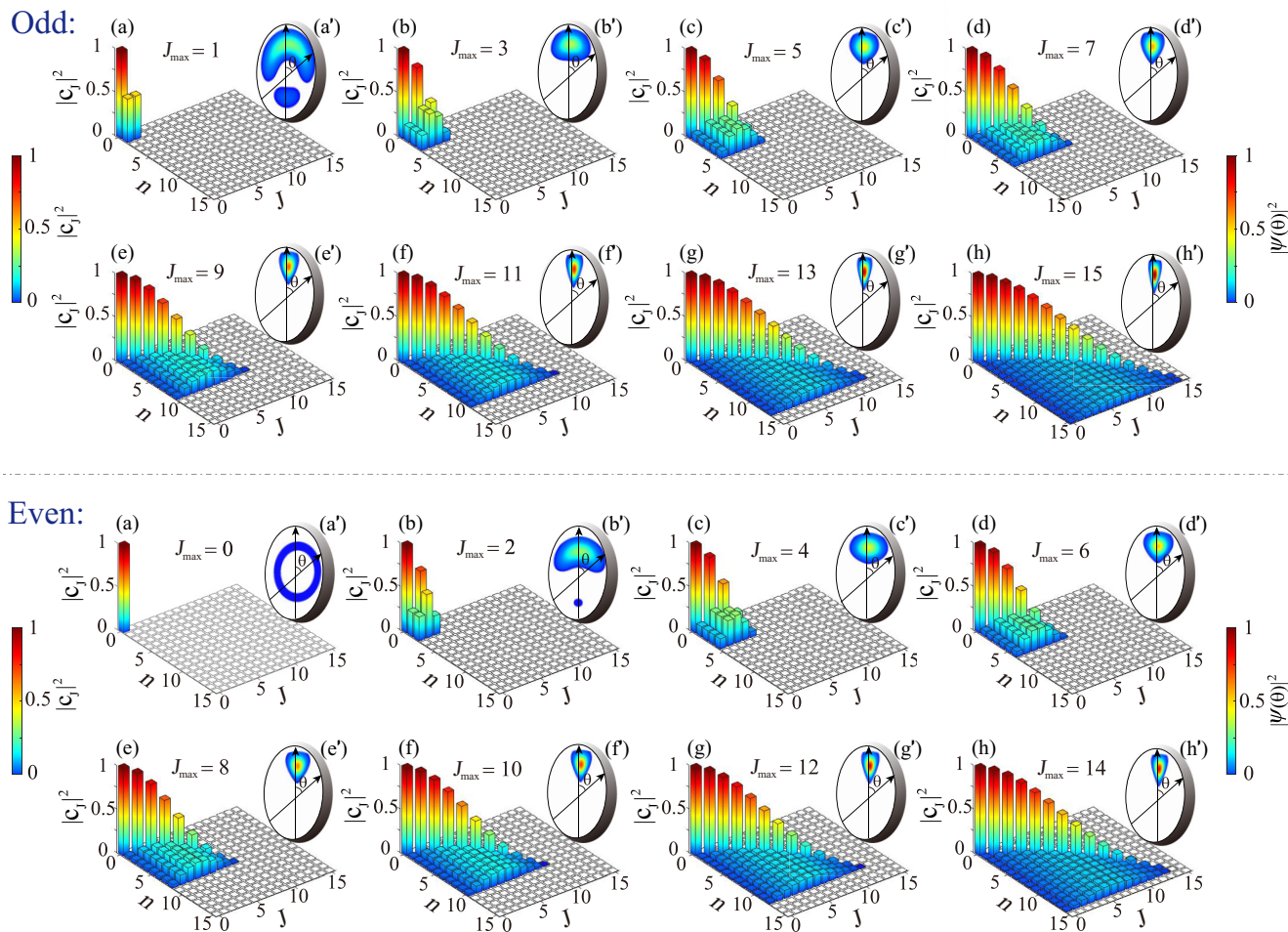
FIG. 3. The population distributions of $|c_J|^2$ (a)–(h) and the corresponding angular distributions of the rovibrational wave packets (a')–(h') after the nth subpulse excitation for pulse sequences containing an odd number of subpulses in the upper panels and an even number in the lower panels.

$T_{rot} = \pi/B = 2.2$ ps, as shown in Figs. 2(b) and 2(d). These revivals highlight the periodic nature of rotational dynamics, emphasizing the recurrent patterns in the quantum behavior of the system.

Figure 3 illustrates the corresponding rotational population and wave-packet distributions of molecules after interacting with each subpulse under the different pulse sequences used in Fig. 2. Initially, all molecules start in the same rotational state $|0\rangle$ with $\langle\cos\theta\rangle = 0$. The population transfer from the initial state to higher excited states varies with the number of subpulses for a given pulse sequence. Each subpulse modifies the populations of adjacent rotational states and adjusts their phases. By applying different pulse sequences to molecules, distinct population distributions of rotational states are achieved, resulting in the desired coherent superposition (wave packet) of rotational states, which are in excellent agreement with the theoretical values (listed in Ref. [62]) calculated by using Eq. (8). Since the phases of all rotational states are modulated to the same values as the initial state, i.e., $\varphi_1 - \varphi_0 = 0$ in Eq. (9), all analytically designed pulse sequences in Figs. 2(a) and 2(c) drive the molecules to the positive maximum degree of orientation at the same target time, exhibiting revivals to their maximums at the same

delays, as depicted in Figs. 2(b) and 2(d). Consequently, our simulations clearly demonstrate that these analytically designed pulses can effectively manipulate the rotational motions of molecules, guiding the molecules toward the desired orientation. Our numerical simulations that did not use approximations on the unitary time evolution show excellent agreement with the theoretical predictions, confirming the validity of the analytical pulses derived from the first-order Magnus approximation.

We also examine how the analytically designed pulse sequences in Figs. 2(a) and 2(c) influence the time-dependent degree of alignment $\langle\cos^2\theta\rangle(t)$, as illustrated in Fig. 4. In the case of a single pulse, no even rotational states are excited, so we observe that the alignment maintains a constant value of 0.47, below the theoretical maximum of 0.6. As the number of pulses increases, the degree of alignment improves, and periodic revivals occur. Interestingly, a high alignment value over 0.98 can be obtained by exciting the lowest 16 rotational states. It is important to note that the optimized phases between states used in our simulations to achieve the theoretical maximum orientation are also ideal for attaining the theoretical maximum alignment. To reach the maximum alignment for different values of J_{max}, we need to optimize
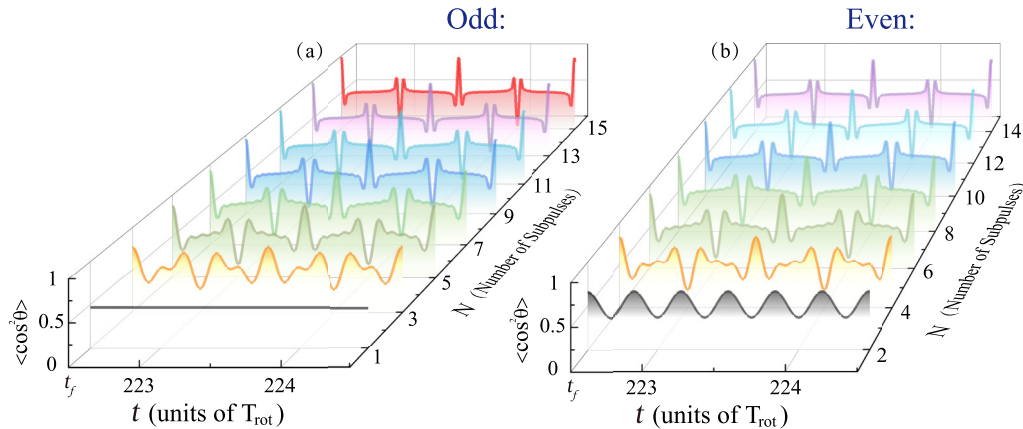
FIG. 4. The degree of alignment $\langle\cos^2\theta\rangle$ for different odd (a) and even (b) numbers of $N = J_{\max}$. The time is measured in units of the full revival period π/B of the molecule. The applied pulse sequences are the same as those used in Fig. 2.

the population distribution of the involved rotational states by only adjusting the strength of each subpulse.

Discussion. Over the past three decades, considerable efforts have been dedicated to generating postpulse orientations [70–73]. These include the development of theoretical models to effectively describe this phenomenon, as well as the design of coherent and optimal control schemes for achieving a high degree of orientation in different molecules [74–79]. The method being used here requires the involvement of resonant interactions of tailored terahertz or microwave pulses with the permanent dipole moment of the molecule, in contrast to the nonresonant interactions of strong laser pulses with the polarizability and hyperpolarizability [80–83]. Advanced terahertz and microwave pulse-shaping techniques, such as amplitude modulation, frequency modulation, and pulse width modulation, can create desired pulse sequences [84–90]. It is also necessary to prepare and measure molecules in specific rovibronic and hyperfine states. Several experimental works have demonstrated the capability to prepare ultracold molecules in their absolute ground state [91–93]. Therefore, two necessary conditions required for the realization of this theoretical proposal are technically available. Additionally, the peak intensity of the applied pulse sequence (less than $2.65 \times 10^5 \, \text{W/cm}^2$ for LiH molecules) is considerably lower than that utilized in nonresonant optical excitation schemes. This indicates that electronic excitation or ionization resulting from nonlinear effects could be negligible.

The maximum degree of orientation achieved depends on the involved number of rotational states, which in turn determines the required number of subpulses. Increasing subpulses may lead to molecules susceptible to the negative effects of quantum decoherence on the phases of rotational states. Additionally, including high-lying rotational states may lead to non-negligible coupling of molecular vibrations to the rotational motions [94]. By taking into account the centrifugal distortion term into the Hamiltonian, we find that the effect of this term was less than 10^{-3} for $J_{\max} = 15$ and is therefore not considered in our simulations. The optimal pulse sequence consisting of 15 subpulses has led to a maximum degree of orientation $|\langle\cos\theta\rangle|_{\max} > 0.99$, which is adequate for practical applications [95]. For the desired target of $J_{\max} > 15$, we

can extend the theoretical method to incorporate the centrifugal distortion term by adjusting the pulse center frequencies while keeping the other variables unchanged.

The present method is universally applicable to different diatomic, linear, and polyatomic molecules at ultracold temperatures [62], whose values of the rotational constants and the permanent dipole moments determine the amplitude and central frequency of each subpulse. There are no added complexities in the optimal pulse sequence for polyatomic nonlinear molecules initially in the absolute ground state ($\nu = 0$ and $J = 0$).

The successful application of this analytical method to precise quantum control of molecular rotation not only showcases its ability to attain maximum molecular orientation values but also underscores its versatility across 15 different scenarios, resulting in the generation of 15 distinct and desired superposition states. These results highlight the potential of applying the proposed analytical approach to precisely construct a desired coherent superposition within a defined subspace of quantum states. In commonly used qubit schemes, one of the main challenges is achieving scalability [96]. This entails engineering a considerable number of individually controllable qubits within a large Hilbert space that is protected from external perturbations and losses. To address this scalability problem, higher-dimensional quantum systems, known as qudits, have been explored as an alternative to qubits [97–99]. Comparing the same size of the Hilbert space, the number of N-level qudits needed is notably smaller than the number of qubits, typically reduced by a factor of $\log_2 N$ [29]. The optimized pulse sequence in Eq. (5) in principle can be potentially applied to the production of qudit gates consisting of multiple quantum states with high fidelity.

Conclusion. We established an analytical method called the multilevel pulse-area theorem to effectively control a specific number of quantum states, enabling the construction of desired superpositions of rotational states in molecules. Our results demonstrated how the analytically designed laser pulse sequences can be accurately mapped onto the rotational states within a given subspace. To illustrate this method, we conducted numerical simulations to precisely control ultracold polar molecules. The analytically designed pulse sequences

can optimize the distribution of rotational populations and the relative phases between adjacent rotational states, leading to the desired molecular orientation. The realization of this theoretical proposal is promising by using current terahertz and microwave pulse-shaping techniques.

The potential application of this analytical framework extends beyond merely achieving maximum molecular orientation. It offers an alternative method for precisely controlling a specific number of rotational states, ultimately enabling the creation of any desired rotational superposition. This capability is vital for utilizing molecular-based qubit, qutrit, and qudit systems in quantum information techniques. This work is essential for preparing high-fidelity coherent superpositions of higher-dimensional quantum states, which has important implications for precision spectroscopy, quantum computing, and quantum information storage and processing in molecules.

[1] D. DeMille, Quantum computation with trapped polar molecules, Phys. Rev. Lett. **88**, 067901 (2002).

[2] I. Manai, R. Horchani, H. Lignier, P. Pillet, D. Comparat, A. Fioretti, and M. Allegrini, Rovibrational cooling of molecules by optical pumping, Phys. Rev. Lett. **109**, 183001 (2012).

[3] K. Wang, C. P. Williams, L. R. B. Picard, N. Y. Yao, and K.-K. Ni, Enriching the quantum toolbox of ultracold molecules with Rydberg atoms, PRX Quantum **3**, 030339 (2022).

[4] Y. Bao, S. S. Yu, L. Anderegg, E. Chae, W. Ketterle, K.-K. Ni, and J. M. Doyle, Dipolar spin-exchange and entanglement between molecules in an optical tweezer array, Science **382**, 1138 (2023).

[5] A. S. Chatterley, C. Schouder, L. Christiansen, B. Shepperson, M. H. Rasmussen, and H. Stapelfeldt, Long-lasting field-free alignment of large molecules inside helium nanodroplets, Nat. Commun. **10**, 133 (2019).

[6] C. P. Koch, M. Lemeshko, and D. Sugny, Quantum control of molecular rotation, Rev. Mod. Phys. **91**, 035005 (2019).

[7] E. J. Zak, A. Yachmenev, and J. Küpper, Controlling rotation in the molecular frame with an optical centrifuge, Phys. Rev. Res. **3**, 023188 (2021).

[8] T. Mullins, E. T. Karamatskos, J. Wiese, J. Onvlee, A. Rouzée, A. Yachmenev, S. Trippel, and J. Küpper, Picosecond pulse-shaping for strong three-dimensional field-free alignment of generic asymmetric-top molecules, Nat. Commun. **13**, 1431 (2022).

[9] J. Qiang, L. Zhou, P. Lu, K. Lin, Y. Ma, S. Pan, C. Lu, W. Jiang, F. Sun, W. Zhang *et al.*, Femtosecond rotational dynamics of D_2 molecules in superfluid helium nanodroplets, Phys. Rev. Lett. **128**, 243201 (2022).

[10] A. A. Milner, I. MacPhail-Bartley, K. Preocanin, S. Dasgupta, X. Peng, and V. Milner, Coherent control of molecular rotation in superfluid helium, Phys. Rev. A **109**, 013110 (2024).

[11] M. Machholm and N. E. Henriksen, Field-free orientation of molecules, Phys. Rev. Lett. **87**, 193001 (2001).

[12] K. Oda, M. Hita, S. Minemoto, and H. Sakai, All-optical molecular orientation, Phys. Rev. Lett. **104**, 213901 (2010).

[13] S. Fleischer, Y. Zhou, R. W. Field, and K. A. Nelson, Molecular orientation and alignment by intense single-cycle THz pulses, Phys. Rev. Lett. **107**, 163603 (2011).

[14] K. N. Egodapitiya, S. Li, and R. R. Jones, Terahertz-induced field-free orientation of rotationally excited molecules, Phys. Rev. Lett. **112**, 103002 (2014).

[15] K. Lin, I. Tutunnikov, J. Qiang, J. Ma, Q. Song, Q. Ji, W. Zhang, H. Li, F. Sun, X. Gong *et al.*, All-optical field-free three-dimensional orientation of asymmetric-top molecules, Nat. Commun. **9**, 5134 (2018).

[16] L. Xu, I. Tutunnikov, E. Gershnabel, Y. Prior, and I. S. Averbukh, Long-lasting molecular orientation induced by a single terahertz pulse, Phys. Rev. Lett. **125**, 013201 (2020).

[17] L.-B. Fan, C.-C. Shu, D. Dong, J. He, N. E. Henriksen, and F. Nori, Quantum coherent control of a single molecular-polariton rotation, Phys. Rev. Lett. **130**, 043604 (2023).

[18] S. A. Moses, J. P. Covey, M. T. Miecnikowski, D. S. Jin, and J. Ye, New frontiers for quantum gases of polar molecules, Nat. Phys. **13**, 13 (2017).

[19] S. Fukahori, T. Otobe, H. Akagi, K. Yamanouchi, and R. Itakura, Orientation-angle-resolved photoelectron angular distribution in dissociative ionization of methanol induced by an intense ultraviolet laser pulse, Phys. Rev. A **107**, 053118 (2023).

[20] I. D. Leroux, M. H. Schleier-Smith, and V. Vuletić, Orientation-dependent entanglement lifetime in a squeezed atomic clock, Phys. Rev. Lett. **104**, 250801 (2010).

[21] S. Alighanbari, M. G. Hansen, V. Korobov, and S. Schiller, Rotational spectroscopy of cold and trapped molecular ions in the Lamb–Dicke regime, Nat. Phys. **14**, 555 (2018).

[22] W. Siu, F. Kelkensberg, G. Gademann, A. Rouzée, P. Johnsson, D. Dowek, M. Lucchini, F. Calegari, U. De Giovannini, A. Rubio *et al.*, Attosecond control of dissociative ionization of O_2 molecules, Phys. Rev. A **84**, 063412 (2011).

[23] J. Li, Q. Zhang, L. Li, X. Zhu, T. Huang, P. Lan, and P. Lu, Orientation dependence of high-order harmonic generation in nanowire, Phys. Rev. A **99**, 033421 (2019).

[24] J. Zhou, C. He, M.-M. Liu, E. Wang, S. Jia, A. Dorn, X. Ren, and Y. Liu, Real-time observation of ultrafast molecular rotation in weakly bound dimers, Phys. Rev. Res. **3**, 023050 (2021).

[25] D. V. Rezvan, K. Klyssek, S. Grundmann, A. Pier, N. M. Novikovskiy, N. Strenger, D. Tsitsonis, M. Kircher, I. Vela-Peréz, K. Fehre, F. Trinter, M. S. Schöffler, T. Jahnke, R. Dörner, and P. V. Demekhin, Observation of nondipole-induced asymmetry in the angular emission distribution of photoelectrons from fixed-in-space CO molecules, Phys. Rev. Lett. **129**, 253201 (2022).

[26] J. D. Pickering, B. Shepperson, B. A. K. Hübschmann, F. Thorning, and H. Stapelfeldt, Alignment and imaging of the CS_2 dimer inside helium nanodroplets, Phys. Rev. Lett. **120**, 113202 (2018).

[27] D. Qi, F. Cao, S. Xu, Y. Yao, Y. He, J. Yao, P. Ding, C. Jin, L. Deng, T. Jia, J. Liang, Z. Sun, and S. Zhang, 100-trillion-frame-per-second single-shot compressed ultrafast photography via molecular alignment, Phys. Rev. Appl. **15**, 024051 (2021).

[28] T. K. Begzjav, Z. Zhang, M. O. Scully, and G. S. Agarwal, Enhanced signals from chiral molecules via molecular coherence, Opt. Express **27**, 13965 (2019).

[29] E. A. Shapiro, M. Spanner, and M. Y. Ivanov, Quantum logic in coarse grained control of wavepackets, J. Mod. Opt. **52**, 897 (2005).

[30] C. Wu, A. B. Khanikaev, R. Adato, N. Arju, A. A. Yanik, H. Altug, and G. Shvets, Fano-resonant asymmetric metamaterials for ultrasensitive spectroscopy and identification of molecular monolayers, Nat. Mater. **11**, 69 (2012).

[31] V. Karle, A. Ghazaryan, and M. Lemeshko, Topological charges of periodically kicked molecules, Phys. Rev. Lett. **130**, 103202 (2023).

[32] J. Zhang, Y.-x. Liu, R.-B. Wu, K. Jacobs, and F. Nori, Quantum feedback: Theory, experiments, and applications, Phys. Rep. **679**, 1 (2017).

[33] V. V. Albert, J. P. Covey, and J. Preskill, Robust encoding of a qubit in a molecule, Phys. Rev. X **10**, 031050 (2020).

[34] K. Mishima and K. Yamashita, Quantum computing using rotational modes of two polar molecules, Chem. Phys. **361**, 106 (2009).

[35] I. M. Georgescu, S. Ashhab, and F. Nori, Quantum simulation, Rev. Mod. Phys. **86**, 153 (2014).

[36] M. Hughes, M. D. Frye, R. Sawant, G. Bhole, J. A. Jones, S. L. Cornish, M. R. Tarbutt, J. M. Hutson, D. Jaksch, and J. Mur-Petit, Robust entangling gate for polar molecules using magnetic and microwave fields, Phys. Rev. A **101**, 062308 (2020).

[37] P. O. Kofman, S. N. Shevchenko, and F. Nori, Tuning the initial phase to control the final state of a driven qubit, Phys. Rev. A **109**, 022409 (2024).

[38] Q. Wei, S. Kais, B. Friedrich, and D. Herschbach, Entanglement of polar symmetric top molecules as candidate qubits, J. Chem. Phys. **135**, 154102 (2011).

[39] J. A. Blackmore, L. Caldwell, P. D. Gregory, E. M. Bridge, R. Sawant, J. Aldegunde, J. Mur-Petit, D. Jaksch, J. M. Hutson, B. Sauer *et al.*, Ultracold molecules for quantum simulation: Rotational coherences in CaF and RbCs, Quantum Sci. Technol. **4**, 014010 (2018).

[40] K.-K. Ni, T. Rosenband, and D. D. Grimes, Dipolar exchange quantum logic gate with polar molecules, Chem. Sci. **9**, 6830 (2018).

[41] P. Yu, L. W. Cheuk, I. Kozyryev, and J. M. Doyle, A scalable quantum computing platform using symmetric-top molecules, New J. Phys. **21**, 093049 (2019).

[42] Z.-Y. Wang and R.-B. Liu, Extending quantum control of time-independent systems to time-dependent systems, Phys. Rev. A **83**, 062313 (2011).

[43] S. J. Glaser, U. Boscain, T. Calarco, C. P. Koch, W. Köckenberger, R. Kosloff, I. Kuprov, B. Luy, S. Schirmer, T. Schulte-Herbrüggen *et al.*, Training Schrödinger's cat: Quantum optimal control: Strategic report on current status, visions and goals for research in Europe, Eur. Phys. J. D **69**, 279 (2015).

[44] C.-W. Chou, C. Kurz, D. B. Hume, P. N. Plessow, D. R. Leibrandt, and D. Leibfried, Preparation and coherent manipulation of pure quantum states of a single molecular ion, Nature (London) **545**, 203 (2017).

[45] S. Kallush, R. Dann, and R. Kosloff, Controlling the uncontrollable: Quantum control of open-system dynamics, Sci. Adv. **8**, eadd0828 (2022).

[46] D. Dong and I. R. Petersen, *Learning and Robust Control in Quantum Technology* (Springer Nature, London, 2023).

[47] L. Dominici, D. Colas, S. Donati, J. P. Restrepo Cuartas, M. De Giorgi, D. Ballarini, G. Guirales, J. C. López Carreño, A. Bramati, G. Gigli, E. del Valle, F. P. Laussy, and D. Sanvitto, Ultrafast control and Rabi oscillations of polaritons, Phys. Rev. Lett. **113**, 226401 (2014).

[48] K. A. Fischer, L. Hanschke, M. Kremser, J. J. Finley, K. Müller, and J. Vučković, Pulsed Rabi oscillations in quantum two-level systems: Beyond the area theorem, Quantum Sci. Technol. **3**, 014006 (2018).

[49] Z.-C. Shi, Y.-H. Chen, W. Qin, Y. Xia, X. X. Yi, S.-B. Zheng, and F. Nori, Two-level systems with periodic *n*-step driving fields: Exact dynamics and quantum state manipulations, Phys. Rev. A **104**, 053101 (2021).

[50] O. V. Ivakhnenko, S. N. Shevchenko, and F. Nori, Nonadiabatic Landau–Zener–Stückelberg–Majorana transitions, dynamics, and interference, Phys. Rep. **995**, 1 (2023).

[51] Y. Guo, X. Gong, S. Ma, and C.-C. Shu, Cyclic three-level-pulse-area theorem for enantioselective state transfer of chiral molecules, Phys. Rev. A **105**, 013102 (2022).

[52] R. Judson, K. Lehmann, H. Rabitz, and W. Warren, Optimal design of external fields for controlling molecular motion: Application to rotation, J. Mol. Struct. **223**, 425 (1990).

[53] J. Ortigoso, Design of tailored microwave pulses to create rotational coherent states for an asymmetric-top molecule, Phys. Rev. A **57**, 4592 (1998).

[54] J. Salomon, C. M. Dion, and G. Turinici, Optimal molecular alignment and orientation through rotational ladder climbing, J. Chem. Phys. **123**, 144310 (2005).

[55] C.-C. Shu, T.-S. Ho, and H. Rabitz, Monotonic convergent quantum optimal control method with exact equality constraints on the optimized control fields, Phys. Rev. A **93**, 053418 (2016).

[56] Y. Guo, X. Luo, S. Ma, and C.-C. Shu, All-optical generation of quantum entangled states with strictly constrained ultrafast laser pulses, Phys. Rev. A **100**, 023409 (2019).

[57] M. Montesinos and A. Pérez-Lorenzana, Exact solutions of *n*-level systems and gauge theories, Phys. Rev. A **60**, 2554 (1999).

[58] E. Groves, B. Clader, and J. Eberly, Multipulse quantum control: Exact solutions, Opt. Lett. **34**, 2539 (2009).

[59] Y. Guo, C.-C. Shu, D. Dong, and F. Nori, Vanishing and revival of resonance Raman scattering, Phys. Rev. Lett. **123**, 223202 (2019).

[60] Q.-Q. Hong, L.-B. Fan, C.-C. Shu, and N. E. Henriksen, Generation of maximal three-state field-free molecular orientation with terahertz pulses, Phys. Rev. A **104**, 013108 (2021).

[61] L.-B. Fan and C.-C. Shu, Pulse-area theorem for precision control of the rotational motions of a single molecule in a cavity, J. Phys. A: Math. Theor. **56**, 365302 (2023).

[62] See Supplemental Material at http://link.aps.org/supplemental/10.1103/PhysRevResearch.7.L012049 for the detailed derivations and additional simulations.

[63] D. Sugny, A. Keller, O. Atabek, D. Daems, C. M. Dion, S. Guérin, and H. R. Jauslin, Reaching optimally oriented molecular states by laser kicks, Phys. Rev. A **69**, 033402 (2004).

[64] S. Wang and N. E. Henriksen, Optimal field-free molecular orientation with nonresonant two-color adiabatic-turn-on and sudden-turn-off laser pulses, Phys. Rev. A **102**, 063120 (2020).

[65] E. S. Shuman, J. F. Barry, and D. DeMille, Laser cooling of a diatomic molecule, Nature (London) **467**, 820 (2010).

[66] C. Chin, R. Grimm, P. Julienne, and E. Tiesinga, Feshbach resonances in ultracold gases, Rev. Mod. Phys. **82**, 1225 (2010).

[67] M. Guo, B. Zhu, B. Lu, X. Ye, F. Wang, R. Vexiau, N. Bouloufa-Maafa, G. Quéméner, O. Dulieu, and D. Wang, Creation of an ultracold gas of ground-state dipolar $^{23}Na^{87}Rb$ molecules, Phys. Rev. Lett. **116**, 205303 (2016).

[68] C.-C. Shu, K.-J. Yuan, W.-H. Hu, and S.-L. Cong, Field-free molecular orientation with terahertz few-cycle pulses, J. Chem. Phys. **132**, 244311 (2010).

[69] S. Trippel, T. Mullins, N. L. M. Müller, J. S. Kienitz, R. González-Férez, and J. Küpper, Two-state wave packet for strong field-free molecular orientation, Phys. Rev. Lett. **114**, 103003 (2015).

[70] R. Tehini, M. Z. Hoque, O. Faucher, and D. Sugny, Field-free molecular orientation of $^1\Sigma$ and $^2\Pi$ molecules at high temperature, Phys. Rev. A **85**, 043423 (2012).

[71] C.-C. Shu and N. E. Henriksen, Field-free molecular orientation induced by single-cycle THz pulses: The role of resonance and quantum interference, Phys. Rev. A **87**, 013408 (2013).

[72] P. M. Kraus, D. Baykusheva, and H. J. Wörner, Two-pulse field-free orientation reveals anisotropy of molecular shape resonance, Phys. Rev. Lett. **113**, 023001 (2014).

[73] J.-P. Zhang, S. Wang, and N. E. Henriksen, Optimal field-free orientation of molecules with resonant tailored multicolor fields, Phys. Rev. A **107**, 033118 (2023).

[74] J. Ortigoso, Conservation of molecular alignment for cyclic rotational wave packets in periodic pulse trains, Phys. Rev. Lett. **93**, 073001 (2004).

[75] K. Nakajima, H. Abe, and Y. Ohtsuki, Optimal control simulation of field-free molecular orientation: Alignment-enhanced molecular orientation, J. Phys. Chem. A **116**, 11219 (2012).

[76] S.-L. Liao, T.-S. Ho, H. Rabitz, and S.-I. Chu, Maximum attainable field-free molecular orientation of a thermal ensemble with near–single-cycle THz pulses, Phys. Rev. A **87**, 013429 (2013).

[77] C. K. M. Ndong and D. Sugny, Time optimization and state-dependent constraints in the quantum optimal control of molecular orientation, J. Mod. Opt. **61**, 857 (2014).

[78] S. Luo, R. Zhu, L. He, W. Hu, X. Li, P. Ma, C. Wang, F. Liu, W. G. Roeterdink, S. Stolte, and D. Ding, Nonadiabatic laser-induced orientation and alignment of rotational-state-selected CH_3Br molecules, Phys. Rev. A **91**, 053408 (2015).

[79] L. Xu, I. Tutunnikov, Y. Prior, and I. S. Averbukh, Enhanced persistent orientation of asymmetric-top molecules induced by cross-polarized terahertz pulses, Phys. Rev. Res. **6**, 013201 (2024).

[80] M. Spanner, S. Patchkovskii, E. Frumker, and P. Corkum, Mechanisms of two-color laser-induced field-free molecular orientation, Phys. Rev. Lett. **109**, 113001 (2012).

[81] I. Znakovskaya, M. Spanner, S. De, H. Li, D. Ray, P. Corkum, I. V. Litvinyuk, C. L. Cocke, and M. F. Kling, Transition between mechanisms of laser-induced field-free molecular orientation, Phys. Rev. Lett. **112**, 113005 (2014).

[82] R. Damari, S. Kallush, and S. Fleischer, Rotational control of asymmetric molecules: Dipole- versus polarizability-driven rotational dynamics, Phys. Rev. Lett. **117**, 103001 (2016).

[83] Q.-Q. Hong, Z.-Z. Lian, C.-C. Shu, and N. E. Henriksen, Quantum control of field-free molecular orientation, Phys. Chem. Chem. Phys. **25**, 32763 (2023).

[84] D. Goswami, Optical pulse shaping approaches to coherent control, Phys. Rep. **374**, 385 (2003).

[85] J. Yao, Photonic generation of microwave arbitrary waveforms, Opt. Commun. **284**, 3723 (2011).

[86] S. Zhdanovich, A. A. Milner, C. Bloomquist, J. Floß, I. S. Averbukh, J. W. Hepburn, and V. Milner, Control of molecular rotation with a chiral train of ultrashort pulses, Phys. Rev. Lett. **107**, 243004 (2011).

[87] J. T. Merrill and K. R. Brown, Progress in compensating pulse sequences for quantum computation, Adv. Chem. Phys. **154**, 241 (2014).

[88] Z. Zeng, L. Zhang, Y. Zhang, H. Tian, Z. Zhang, S. Zhang, H. Li, and Y. Liu, Microwave pulse generation via employing an electric signal modulator to achieve time-domain mode locking in an optoelectronic oscillator, Opt. Lett. **46**, 2107 (2021).

[89] J. E. Nkeck, L.-P. Béliveau, X. Ropagnol, D. Deslandes, D. Morris, and F. Blanchard, Parallel generation and coding of a terahertz pulse train, APL Photonics **7**, 126105 (2022).

[90] X. Zhou, Y. Lin, Y. Chan, F. Deng, and J. Zhang, Coherent generation and control of tunable narrowband THz radiation from a laser-induced air-plasma filament, Opt. Lett. **48**, 2881 (2023).

[91] F. Seeßelberg, N. Buchheim, Z.-K. Lu, T. Schneider, X.-Y. Luo, E. Tiemann, I. Bloch, and C. Gohle, Modeling the adiabatic creation of ultracold polar $^{23}Na^{40}K$ molecules, Phys. Rev. A **97**, 013405 (2018).

[92] H. Yang, J. Cao, Z. Su, J. Rui, B. Zhao, and J.-W. Pan, Creation of an ultracold gas of triatomic molecules from an atom–diatomic molecule mixture, Science **378**, 1009 (2022).

[93] T. Langen, G. Valtolina, D. Wang, and J. Ye, Quantum state manipulation and cooling of ultracold molecules, Nat. Phys. **20**, 702 (2024).

[94] L. Yuan, S. W. Teitelbaum, A. Robinson, and A. S. Mullin, Dynamics of molecules in extreme rotational states, Proc. Natl. Acad. Sci. USA **108**, 6872 (2011).

[95] D. Daems, S. Guérin, D. Sugny, and H. R. Jauslin, Efficient and long-lived field-free orientation of molecules by a single hybrid short pulse, Phys. Rev. Lett. **94**, 153003 (2005).

[96] Y. Wang, Z. Hu, B. C. Sanders, and S. Kais, Qudits and high-dimensional quantum computing, Front. Phys. **8**, 589504 (2020).

[97] L. Neves, G. Lima, J. G. Aguirre Gómez, C. H. Monken, C. Saavedra, and S. Pádua, Generation of entangled states of qudits using twin photons, Phys. Rev. Lett. **94**, 100501 (2005).

[98] R. Sawant, J. A. Blackmore, P. D. Gregory, J. Mur-Petit, D. Jaksch, J. Aldegunde, J. M. Hutson, M. R. Tarbutt, and S. L. Cornish, Ultracold polar molecules as qudits, New J. Phys. **22**, 013027 (2020).

[99] M. Ringbauer, M. Meth, L. Postler, R. Stricker, R. Blatt, P. Schindler, and T. Monz, A universal qudit quantum processor with trapped ions, Nat. Phys. **18**, 1053 (2022).